Steady-State Impurity Control, Heat Removal and Tritium Recovery by Moving-Belt Plasma-Facing Components

Y. Hirooka, M. S. Tillack and A. Grossman
Fusion Energy Research Program
University of California, San Diego
9500 Gilman Dr., La Jolla, CA 92093-0417, U. S. A.

Abstract - Discussed in this paper is the application of "Moving-Belt Plasma-Facing Components" for steady-state impurity gettering, heat removal and tritium recovery in fusion reactors. To minimize MHD effects as well as induced radioactivity, semi-metallic or semi-conductor materials such as C-C composite or SiC-SiC composite fabrics are proposed as the belt materials.

I. INTRODUCTION

It is widely recognized that power and particle control is a critical issue, affecting the overall performance of fusion devices. To resolve this issue, the radiative divertor concept has been examined in several fusion devices, injecting inert gases as radiators. The results indicate a substantial heat load reduction onto the divertor plate [1].

However, materials net erosion may increase due to the reduced redeposition efficiency of radiation-cooled plasmas and also due to radiator gas sputtering. For example, the lifetime of a hypothetical 5 mm thick beryllium plate has been estimated to be only 6 hours for a 100% duty cycle under ITER-relevant divertor conditions [2]. The hesitation to use high-Z materials, which are believed to be longer lifetime, comes from the radiation loss effect, an issue that it would no doubt take decades of world-wide effort to resolve.

Turning to wall conditioning and its effects on plasma confinement, there have been several breakthroughs over the past two decades. In TFTR, the super-shot regime was enabled by helium discharge conditioning [3]. The VH-mode in DIII-D was achieved by combined helium glow discharge and boronization [4]. Recently, lithium wall conditioning has brought the enhanced supershot regime in TFTR during the recent DT campaign [5].

The key for these successful wall conditioning techniques is the achievement of reduced particle recycling. However, by nature the wall conditioning effect has finite lifetime because the surface is saturable and coatings will be eroded. Once lifetime is reached either way, the wall must be reconditioned. Clearly, this is not desirable to future steady-state fusion reactors.

As an attempt to resolve this wall saturation issue, STB (Solid-Target Boronization) was demonstrated in several fusion devices [6]. Results successfully demonstrated non-saturable recycling control due to particles co-deposition. However, codeposition leads to the continuous build-up of tritium, an environmental safety issue for a power reactor.

II. MOVING-BELT PFC

To review innovative PFC concepts, in 1974 the liquid lithium divertor was proposed in the UWMAK-I reactor study [7]. However, the critical issue was the handling of MHD effects under high magnetic fields. In 1982, the rotating drum divertor concept was investigated in the UWTOR-M reactor study [8]. In this concept, a radiatively-cooled graphite shell rotates at 1500°C under plasma bombardment. However, at these temperatures graphite is subjected to high-rate erosion due to radiation-enhanced sublimation, which was not yet discovered back then. In 1993, the fully toroidal moving-belt plasma-facing component (MB-PFC) concept was once proposed to extend the erosion lifetime, using metallic materials for the belt, but ended up raising the MHD issue, again [9].

Proposed in the present work is the use of MB-PFCs in combination with external inline belt processing systems, as shown in Fig. 1, for continuous coating of low-Z getter materials, heat removal and tritium recovery. In order to minimize MHD effects as well as induced radioactivity, semi-metallic or semi-conductor materials such as C-C or SiC-SiC fiber fabrics are proposed to use for the belt. These fibers are woven without binder, so that the resultant fabrics remain flexible. To compensate for the gas leak through the belt openings, the inline systems may be housed in a low vacuum enclosure. Clearly, MB-PFCs can be used for all types of magnetic fusion devices. *Most importantly, one can benefit from MB-PFCs without full toroidal application* because, if gettered, the moving-belt surface can act as a non-saturable impurity "drainage".

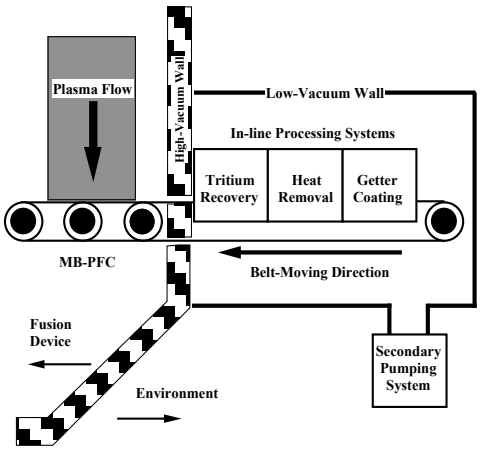

Fig. 1 The moving-belt PFC concept with ex-situ inline belt processing systems for tritium recovery, heat removal and getter coatings.

III. MB-PFCs PERFORMANCE EVALUATION

A. Impurity Control Scenario

For a stationary (non-moving) surface, the net erosion rate under DT-plasma bombardment is given by the following equation, taking into account the effect of redeposition:

$$\Gamma_{net} \cong \frac{(1 - P_{redep.})\Gamma_{gross}}{1 - P_{redep.} Y_{ss}}, \quad (1)$$

where $\Gamma_{gross} = \Gamma_D Y_D + \Gamma_T Y_T + \Sigma \Gamma_i Y_i$ (2)

$(\Gamma_D + \Gamma_T) >> \Sigma \Gamma_i$, (3)

Γ_{net} is the net erosion, $P_{redep.}$ is the redeposition probability, Y_{ss} is the self-sputtering yield, Γ_{gross} is the gross erosion rate, Γ_D and Γ_T are the deuterium and tritium fluxes, Y_D and Y_T are the deuterium and tritium sputtering yields, respectively, Γ_i is the flux of plasma impurity-i and Y_i is the sputtering yield by impurity-i.

The net erosion rate for a moving-belt can be related to that for a stationary surface in the following manner:

$$\Gamma_{MB\text{-}net} = \Gamma_{net} (l_1/L) \quad (4)$$

where $\Gamma_{MB\text{-}net}$ is the moving belt erosion rate, l_1 is the plasma interaction length and L is the total belt length. Notice from eq. (3) that the erosion rate is "diluted" over the moving surface by a factor of (l_1/L). *Interestingly, the erosion rate is independent of the belt moving speed.*

In order to provide an active impurity control capability and further extended lifetime, the moving belt is proposed to be coated with low-Z getters. The candidate getters are lithium, beryllium and boron because the gettering efficiencies for oxygen and carbon are essentially 100% at energies between 50 and 500 eV, calculated from the TRIM-SP code [10]. Using an evaporation source for film deposition, the evaporation rate is given as follows:

$$\Gamma_{evap.} = \frac{P_{eq.}}{\sqrt{2\pi m k T_s}} \quad (5)$$

where T_s is the evaporation source temperature, $P_{eq.}$ is the equilibrium vapor pressure, m is the molecular weight, and k is the Boltzman constant. The film deposition rate over a moving belt is given by the following equation:

$$\Gamma_{MB\text{-}depo.} = \Gamma_{evap.} (l_2/L) \nu \phi(\vartheta) \quad (6)$$

where $\Gamma_{MB\text{-}depo.}$ is the deposition rate on a moving belt, ν is the sticking coefficient, l_2 is the length of the coating section, $\phi(\vartheta)$ is the correction factor for the solid angle, ϑ, viewing from the evaporation source to the belt surface. Deposition rates estimated from eq. (6) are shown in Fig. 2. If the rates of erosion and deposition are balanced, *the getter-coated moving-belt will have an unlimited lifetime with an active impurity control capability.*

B. Erosion-Deposition Balanced Condition

To evaluate whether or not a "zero-erosion" condition can be attained at a practical evaporation source temperature, using the data shown in Fig. 2, case studies have been carried out under the MB-PFC operating conditions listed in Table 1. Here, the carbon belt erosion is not considered because the masking effect is expected from getter coatings. For sputtering yield calculations, the normal incidence of 100% deuterium plasmas is assumed for simplicity.

(1) Li-getter: ${}_{Li}Y_D = 0.04$, ${}_{Li}Y_O = 0.2$, and ${}_{Li}Y_{ss} = 0.1$ and $\Gamma_{MB\text{-}net} = 1.3 \times 10^{16}$ Li-atoms/cm^2/s. To balance erosion loss, the evaporation source must operate at $T_s > 450$ °C.

(2) Be-getter: ${}_{Be}Y_D = 0.043$, ${}_{Be}Y_O = 0.13$, ${}_{Be}Y_{ss} = 0.14$ and $\Gamma_{MB\text{-}net} = 1.5 \times 10^{16}$ Be-atoms/cm^2/s. To balance erosion loss, the evaporation source must operate at $T_s > 1100$ °C.

(3) B-getter: ${}_{B}Y_D = 0.04$, ${}_{B}Y_O = 0.25$, ${}_{B}Y_{ss} = 0.3$ and $\Gamma_{MB\text{-}net} = 1.5 \times 10^{16}$ B-atoms/cm^2/s. To balance erosion loss, the evaporation source must operate at $T_s > 2000$ °C.

All these conditions are achievable with commercially available evaporation sources. The materials loss by evaporation during plasma exposure is assumed to be small, compared with that by sputtering, because the redeposition efficiency for thermal neutrals is nearly 100%.

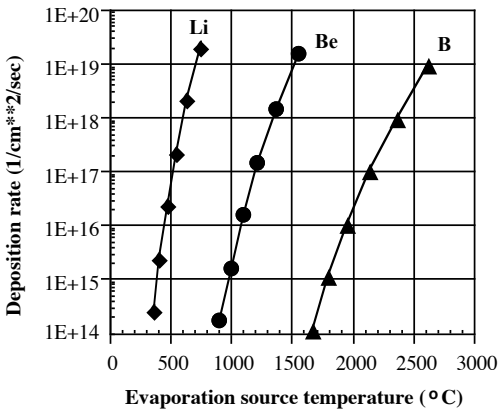

Fig. 2 Estimated getter material deposition rates onto a moving belt.

Table 1 MB-PFC system operating conditions and belt properties*.

Belt length, L	20 m
Belt width, W	1m
Belt thickness, t_b	1 mm
Belt density, ρ	2.2 g/cm^3
Belt speed, v_b	2 m/s
Plasma interaction length, l_1	1 m
Tritium recovery section length, l_T	2 m
Getter-coating section length, l_2	2 m
Fuel plasma fluxes, $\Gamma_D + \Gamma_T$	each 0.995A/cm^2
Oxygen impurity flux, Γ_O	0.01A/cm^2
Particle bombarding energy, E	100 eV
Redeposition probability, P_{redep}	50%
Belt surface temperature	1000 °C
Surface emissivity, ε	0.8
Getter deposition efficiency, $\nu\phi(\vartheta)$	50 %
Thermal conductivity, k	5 W/m-K
Heat capacity, C_p	0.710 J/g-K
Thermal diffusivity, α	0.032 cm^2/s
Stefan-Boltzman constant	5.7x10^{-12} /sW/cm^2-K^4

*Property data for carbon materials are listed here.

B. Heat Removal Options

The primary system for controlling the belt temperature is a heat exchanger located between the hydrogen recovery and getter coating sections. *Three heat removal mechanisms compatible with a low-pressure or vacuum environment have been examined: thermal radiation, contact conductance, and an impinging liquid jet.*

A simple estimate of the area required for heat removal by thermal radiation is shown in Fig. 3. The power removed from a single belt is assumed to be ~2 MW (2 MW/m^2 average over a 1-m^2 exposure area). The emissivity is assumed to be ε=0.8, the view factor is 100%, and the heat sink is kept at room temperature (20˚C). The figure indicates that the belt temperature should be maintained above 800–1000˚C in order to keep the radiator area within reasonable limits. Multiple passes of the belt through the heat exchanger would help enhance the radiator area.

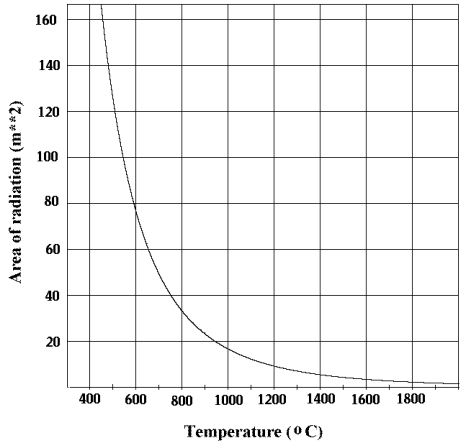

Fig. 3 Area required to remove 2 MW vs. radiator temperature, assuming an emissivity of 0.8 and 100% view factor.

Contact conductance between the belt and roller is another possible heat transfer mechanism. Contact conductance (h) depends strongly on the contact pressure, background gas pressure, and surface characteristics (*e.g.,* roughness and microhardness). In vacuum, the conductance vanishes at zero contact pressure, and is unlikely to exceed ~5000 W/m^2 with moderately smooth surfaces and contact pressure of the order of a few MPa [11]. A background gas pressure of 100 Torr He would add about 5000 W/m^2 additional conductance, but this amount of background gas would require substantial pumping to control the back-flow into the plasma chamber through the belt openings. It seems prudent to rely on the vacuum value of conductance if possible. The area required to remove 2 MW of power is plotted in Fig. 4 vs. the temperature difference between the belt and roller, assuming a contact conductance of 5000 W/m^2. The required area is much more modest for relatively low temperatures. A roller with 1 m radius and 1 m width would be adequate to maintain acceptable temperature drop.

The heat transfer coefficient for a liquid metal jet impinging on a solid surface has been estimated as high

C. Tritium Recovery Efficiency

as 10^5 W/m^2-K [12, 13]. The required area for heat removal would be 20 times smaller than the contact conductance case. This is a very efficient heat transfer mechanism, but is limited in peak temperature by the liquid vapor pressure and by compatibility concerns between the belt and heat transfer loop materials.

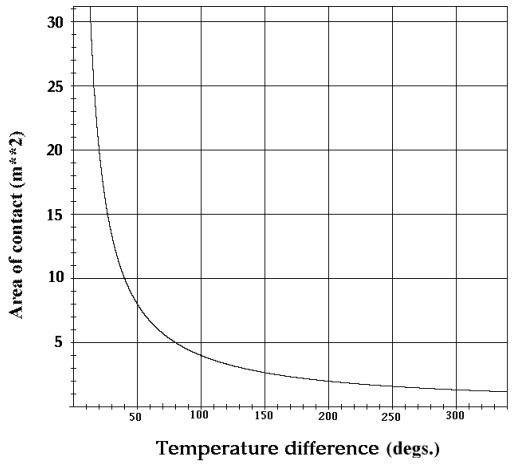

Fig. 4 Area required to remove 2 MW of power vs. temperature difference, assuming contact conductance = 5000W/m$_2$K.

The energy equation for the case of belt motion in the x-direction and conduction in the y-direction was used to determine whether the belt surface temperature would peak much higher than the bulk average temperature. The Nusselt number is plotted in Fig. 5 vs. the Fourier number, where:

$$\mathrm{Fo} = \frac{\tau}{t_b^2 / \alpha} \qquad \mathrm{Nu} = \frac{2ht_b}{k} = \frac{2qt/k}{T_w - T_b} \qquad (7)$$

where τ is the plasma exposure time and α is the thermal diffusivity ($\alpha = k/\rho C_p$). For the conditions listed in Table 1, fully-developed profiles are obtained (Nu=6), and the surface temperature is no more than 133°C higher than the bulk temperature in the exposed region. The bulk temperature rise of the belt across the exposed region is 640˚C.

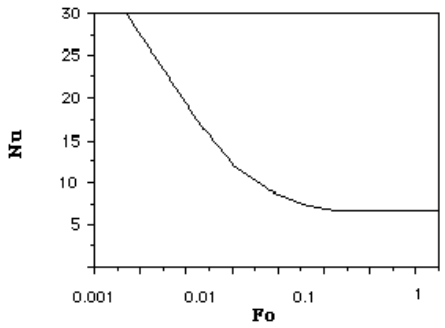

Fig. 5 Heat transfer coefficient expressed by the Nusselt number vs. Fourier number.

Tritium recovery from plasma-facing components affects the fuel economy of reactor operation. Also, tritium inventory in PFCs is a safety issue. Generally, tritium retention in carbonaceous materials decreases as temperature increases [14]. Therefore, as shown in Fig. 1, the tritium recovery section is positioned immediately after plasma exposure in order to take advantage of the heated surface.

To estimate the tritium recovery and inventory, the TMAP code [15] has been run under the conditions listed in Table 1, importing the particle implantation profile information from the TRIM-SP code [10]. The tritium inventory in the carbon belt after n-th rotation, $I_t(n)$, and the recovery efficiency, $\eta(n)$, are defined as follows:

$$I_T(n) = \int_0^{t_b} C_T(x,\ t = t_f)dx \qquad (8)$$

$$\eta(n) = \frac{\Gamma_T l_l / v_b - \{I_T(n) - I_T(n-1)\}}{\Gamma_T l_l / v_b} \qquad (9)$$

where $C_T(x, t)$ is the tritium concentration at the point of x , time of t, and t_f is the time required for one belt rotation.

Shown in Figs. 6 (a) and (b) are the tritium recovery efficiency and inventory as a function of number of belt rotations, respectively. Notice that the recovery efficiency is maintained at 99%, which is considerably higher than the relevant data from TFTR, ranging 10-20% [16]. However, due to the diffusion effect seen as the parabolic behavior in (b), the tritium inventory slowly increases. Assuming that the saturated concentration is 0.2 in terms of (D+T)/C at $T_{av.}$= 720°C (time-averaged temperature over one belt rotation) the maximum tritium inventory is 20g-T/m^2, i.e., 200 kCi/m^2. From parabolic fitting, however, the belt will not be saturated until after 1.8×10^9 rotations, i.e., 570 years, *practically resolving the inventory issue*.

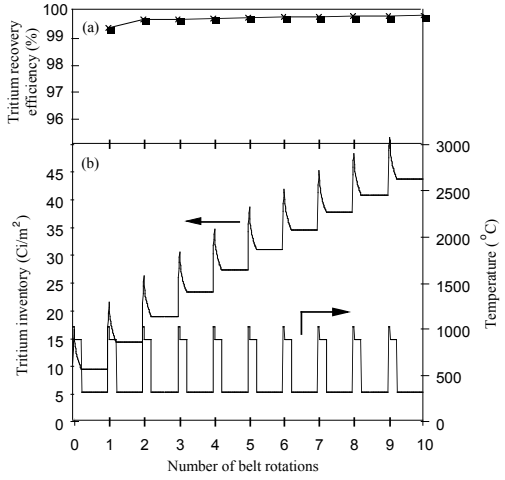

Fig. 6 Tritium recovery efficiency in (a) and, inventory and temperature cycles in (b) over 10 belt rotations (each 10 seconds).

IV. CONCLUSION

The use of MB-PFCs in combination with ex-situ inline belt processing systems has been proposed for future steady-state magnetic fusion reactors. Commercially available C-C or SiC-SiC composite fabrics are considered as the belt materials in order to minimize the complicated MHD effects as well as induced radioactivity. The total system performance has been evaluated under reactor relevant conditions. It is found that the belt erosion loss is diluted over the total belt area and independent of moving speed. Non-saturable impurity gettering is possible under zero-erosion conditions. Heat removal can be carried out continuously either by radiative cooling or contact conductance. Also, the possible use of liquid jet cooling has been discussed under limited conditions. High-efficiency tritium recovery can be maintained for long-term system operation, mitigating the environmental impact.

ACKNOWLEDGEMENTS

Fruitful discussions with R. W. Conn are acknowledged. This work is supported by the U.S. Department of Energy Grants #DE-FG-03-95ER-54301 and 03-95ER54299.

REFERENCES

[1] R. Parker et al., "Plasma-Wall Interactions in ITER", *J. Nucl. Mater.* **241-243**(1997)1-26.
[2] Y. Hirooka et al. "Evaluation of Erosion and Lifetime of ITER Divertor Candidate Materials and Relevant Data from Recent Experiments in the PISCES-B Mod Facility", *Fusion Technol.* **26**(1994)540-545.
[3] J. D. Strachan et al. "Experiments on TFTR Supershot Plasmas" *J. Nucl. Mater.* **176&177**(1990)28-34.
[4] G. L. Jackson et al. "Recycling and Particle Control in DIII-D", *J. Vac. Sci. Technol-A* **10**(1992)1244-1251.
[5] D. K. Mansfield et al. , "Enhancement of Tokamak Fusion Test Reactor Performance by Lithium Conditioning" Phys. Plasmas **3**(1996)1-6.
[6] Y. Hirooka et al., "Solid Target Boronization in the Tokamak de Varennes: A Technique for Real-Time Boronization", *Nucl. Fusion* **32**(1992)2029-2035.
[7] B. Badger et al., "UWMAK-I, A Wisconsin Toroidal Fusion Reactor Design", *University of Wisconsin Report*: UWFDM-68, 1974.
[8] B. Badger et al. "UWTOR-M, A Conceptual Modular Stellarator Power Reactor" *Univ. Wisconsin Report*: UWFDM-550, 1982.
[9] L. Snead and R. A. Vesey, "A Moving Belt Divertor Concept", *Fusion Technol.* **24**(1993)83-96.
[10] J.P. Biersack and W. Eckstein, "Sputtering Studies with the Monte Carlo Program TRIM.SP", *Appl. Phys.* **A34**(1984)73-94.
[11] M. S. Tillack and R. D. Abelson, "Interface Conductance Between Roughened Be and Steel Under Thermal Deformation," *Fusion Eng. and Design* **27**(1995) 232-239.
[12] V. Chuyanov and E. V. Muraviev, "Proposal of Advanced Divertor Plates System Development within ITER EDA," *ITER EDA Memo*, Sep. 1994.
[13] E. Muraviev and the Torus Team, "Liquid Metal Cooled Divertor for ARIES," *General Atomics Report*: GA-A21755, UC-420, Jan. 1995.
[14] R. A. Causey, "The Interaction of Tritium with Graphite and its Impact on Tokamak Operations", *J. Nucl. Mater.* **162-164** (1989)151-161.
[15] G. R. Longhurst, et al. "TMAP4 User's Manual" *INEL Report*:, EGG-FSP-10315 (1992).
[16] D. Mueller, et al. "Removal of Tritium from TFTR", *Fusion Technol.* **30**(1996)840-844.